TRPV4-mediated Ca2+ influx is essential to glomerular endothelial inflammation in sepsis associated acute kidney injury

Xia Wang
Shanghai Chest Hospital: Shanghai Jiao Tong University Affiliated Chest Hospital
Yinhua Wang
Shanghai Chest Hospital: Shanghai Jiao Tong University Affiliated Chest Hospital
Guo Zhou
Shanghai Chest Hospital: Shanghai Jiao Tong University Affiliated Chest Hospital
Yi Li
Shanghai
Huanhuan Huo
Shanghai Chest Hospital: Shanghai Jiao Tong University Affiliated Chest Hospital
Feng Liang
Shanghai Chest Hospital: Shanghai Jiao Tong University Affiliated Chest Hospital
Jieyuan Xue
Shanghai Chest Hospital: Shanghai Jiao Tong University Affiliated Chest Hospital
Xin Shi
Shanghai Chest Hospital: Shanghai Jiao Tong University Affiliated Chest Hospital
Anwen Yin
Shanghai Chest Hospital: Shanghai Jiao Tong University Affiliated Chest Hospital
Qingqing Xiao
Shanghai chest hospital
Linhong Shen
Shanghai Chest Hospital: Shanghai Jiao Tong University Affiliated Chest Hospital
Ben He (heben241@126.com)
Shanghai Chest Hospital: Shanghai Jiao Tong University Affiliated Chest Hospital

Research

Keywords: TRPV4, Ca2+, endothelial cells, sepsis, acute kidney injury

Posted Date: November 5th, 2021

DOI: https://doi.org/10.21203/rs.3.rs-1031344/v1

Abstract

Background

Sepsis-associated acute kidney injury (S-AKI) is a frequent complication of critical patients and is associated with high morbidity and mortality. The glomerular endothelial cell injury is the main characteristics during S-AKI. Ca^{2+} influx is a key step in the establishment of endothelial injury. Transient receptor vanilloid subtype 4 (TRPV4) ion channels are permeable to Ca^{2+} and are widely expressed in endothelial cells. However, the role of TRPV4 on glomerular endothelial inflammation in S-AKI has remained elusive.

Methods

Mouse glomerular endothelial cells (MRGEC) were used to test the molecular mechanism of TRPV4 on LPS-induced glomerular endothelial inflammation. The cecal-ligation-and-puncture (CLP) model was established by ligation of cecum with 4-0 suture and punctured with a 21-gauge needle. Then 0.2mL faeces was extruded from the puncture site to trigger peritoneal inflammation.

Results

In the present study, we found that blocking TRPV4 diminishes LPS-induced cytosolic Ca^{2+}-elevations, which are essential for glomerular endothelial inflammation and barrier function. Furthermore, TRPV4 regulated LPS-induced phosphorylation and translocation of NF-κB and IRF-3 in mouse glomerular endothelial cells (MRGEC). Clamping intracellular Ca^{2+} mimics the LPS-induce response seen in the absence of TRPV4. In vivo, pharmacological blockade or knock down of TRPV4 reduced the inflammatory response of glomerular endothelial cells, inhibited translocation of NF-κB and IRF-3, increased survival rate and improved renal function in CLP-induced sepsis but without altering renal cortical blood perfusion.

Conclusions

Taken together, these results suggested that inhibition of TRPV4 ameliorates glomerular endothelial inflammation, kidney dysfunction, and increased mortality via mediating Ca^{2+} overload and NF-κB/IRF-3 activation. These discoveries may provide novel pharmacological strategies for the treatment of glomerular endothelial dysfunction and kidney injury during endotoxemia, sepsis, and other inflammatory diseases.

Introduction

Sepsis is a life threatening clinical syndrome characterized by organ dysfunction caused by maladaptive host response to infection. Acute kidney injury (AKI) is a frequent complication of sepsis, and ranks as the tenth cause of mortality in the US, especially in patients admitted to the intensive care unit (ICU)(12). Moreover, 35–65% of ICU patients suffered from AKI (24, 28). The impairment of the glomerular filtration barrier (GFB), which is composed of glomerular endothelium, the glomerular basement membrane (GBM) and the podocyte layer is the most important clinical feature of AKI(29). The glomerular endothelium is a semipermeable membrane formed by glomerular endothelial cells (GECs), which are a cell type with round shape and fenestrations(26).Glomerular endothelial cells are susceptible to be damaged by circulating pathogens, endotoxins, proinflammatory cytokines, and reactive oxygen. Previous studies have shown that glomerular endothelial inflammation occurs in the early stage of sepsis(37). Thus, the damage of GECs seems to play a pivotal role in S-AKI.

TRPV4, a Ca^{2+} permeable cation channel, can be activated by diverse stimuli including moderate heat, cell swelling and endogenous and exogenous ligands(18, 38, 39). Our previous study demonstrated that TRPV4-mediated Ca^{2+} rise induces the increase of nitric oxide(NO) production in the mesenteric artery endothelial cells, resulting in a restoration of flow-induced dilation in mesenteric arteries of aged rats(10). In airway epithelial cells, TRPV4-deficient mice display exacerbated ventilatory changes and recruitment of polymorphonuclear leukocytes into the airways after LPS challenge (1). TRPV4 can also regulate vascular permeability in acute lung injury(5). Excessive activation of TRPV4 causes endothelial detachment from the basement membrane, which leads to disruption of the pulmonary endothelial barrier, pulmonary edema, and alveolar flooding(3). Furthermore, pharmacological inhibition of TRPV4 channels reduce cytokine production, restore endothelial function and increase survival in septic mice(9).

Despite the association of TRPV4 function with key characteristics of sepsis, including systemic inflammatory responses, endothelial dysfunction and survival rate, the molecular mechanism of TRPV4 channels involving in the development of S-AKI is unknown. Here we investigated the contribution of TRPV4 channels to the development of S-AKI, and determined whether pharmacological blockade or knock down of TRPV4 exerts a protective effect. In this study, we provide the first evidence that blocking TRPV4 diminishes LPS-induced cytosolic Ca^{2+}-elevations, which are essential for glomerular endothelial inflammation and barrier function. Furthermore, inhibition of TRPV4 restrains NF-κB and IRF-3 nuclear translocation. Clamping intracellular Ca^{2+} mimics the LPS response seen in the absence of TRPV4. In vivo, pharmacological blockade or knock down of TRPV4 reduced the inflammatory response of glomerular endothelial cells, increased survival rate and improved renal function in cecal-ligation-and-puncture (CLP)-induced sepsis without altering renal cortical blood perfusion and NO production. Since TRP channels are highly attractive drug targets(25), these discoveries may provide novel pharmacological strategies for the treatment of glomerular endothelial inflammation and kidney injury during endotoxemia, sepsis, and other inflammatory diseases.

Material And Methods

Animals

C57BL/6 mice(age 6-10weeks,weigh 20-30g, male) were purchased from the Shanghai Jiesijie Experimental Animal Co., Ltd. (Shanghai, China). All the animals were acclimatized in a room (12/12 h light/dark cycle; 25 ± 2°C) and allowed free access to diet and water. All animal experiments were approved by Medical Ethics Committee of Shanghai Jiaotong University, and were performed in strict accordance with approved guidelines.

Mice models

Mice were anesthetized with isoflurane and then randomly divided into control, CLP, HC and CLP+HC groups or NCsiRNA, NCsiRNA+CLP and TRPV4siRNA+CLP groups. The cecum was ligated with 4-0 suture and punctured with a 21-gauge needle. 0.2ml faeces was extruded from the puncture sites. All mice were received 1mL 0.9% normal saline subcutaneously after CLP for fluid resuscitation.

Cell culture

The MRGEC was purchased from Creative Bioarray (NY, USA). Cells were cultured in Dulbecco's modified Eagle medium (DMEM, 4.5 g/L glucose) (Life Technologies, USA) supplemented with 10% fetal bovine serum and antibiotics (100 KU/L penicillin and 100 mg/L streptomycin) in an incubator at 37°C with 5% CO_2.

Western blotting

Protein was extracted from cultured cell lysates with RIPA lysis buffer with phosphatase inhibitor (Roche). The protein concentration was determined by BCA protein concentration assay kit. Equal amounts(30-50μg) proteins were subjected to 12% SDS-PAGE and transferred to PVDF membrane. The membrane was blocked with 5% fat free milk at room temperature for 1 hour and incubated by following primary antibodys: ICAM1 (1:1000, Cell Signaling,

USA), VCAM1 (1:1000, Cell Signaling, USA), E-selectin (1:1000, Cell Signaling, USA), eNOS(1:1000), p-eNOS(1:1000, Cell Signaling, USA), NF-κB(1:1000, Cell Signaling,

USA), IκBα(1:1000, Cell Signaling, USA), p-NF-κB(1:1000, Cell Signaling, USA),IRF-3(1:1000, Beyotime, China),p-IRF-3(1:1000, Beyotime, China) at 4℃ overnight. On the second day, after a 1-hour incubation with HRP-conjugated secondary antibodies, the labeled proteins were detected by ECL(enhanced chemiluminescence). Image analysis was performed by Amersham Image680 Scanning machine and quantified intensity with Image J. The optical density was normalized to that of β-actin(1:1000, Beyotime, Haimen, China), which represented as relative optical density.

Renal histology

Kidney tissues of each group were harvested 24 hours after CLP. The samples were washed with PBS, fixed with 4% paraformaldehyde overnight, embedded in paraffin and cut into sections. Sections were stained with hematoxylin and eosin(HE). HE staining was semi-quantitatively graded under microscopy at

200× to evaluate tissue damage. The grader of the histology slides was examined blindly by a pathologist. The percentage of histological changes in the cortex and medulla was scored using a semi-quantitative scale designed to evaluate the degree of the necrosis in tubular and glomerular areas, tubular vacuolization and cast formation on a five point scale based on injury area of involvement as previous study(7). The scale is as follows: 0≤10%; 1=10-25%; 2=25-50%; 3=50-75%; and 4=75-100%.

Immunohistochemistry

The kidney tissues were fixed with 4% formalin, embedded in paraffin and cut into slices. The sections were incubated with the primary antibodies, ICAM1 (1:1000, Abcam, USA), (E-selectin, 1:100; Beyotime, Haimen, China). Every mouse kidney sample was stained in one slide, and ten viewing fields of the cortex in each slide at 200x magnification were randomly captured for next calculation. The positive cell count of one viewing field in glomerulus was calculated by Image J.

Immunofluorescence staining

Mice were anesthetized with isoflurane and perfused through the left ventricle with normal saline followed by 4% paraformaldehyde. After perfusion, kidney tissues were dissected and cut

into sections at 10 μm with Leica freezing microtome. Slices were washed with 0.01 M of PBS and blocked in 2% BSA for 1 hours at room temperature. After blocking, slices were incubated with primary antibody: anti-CD68(1:100, Abcam, USA), anti-NF-κB(1:100, Cell Signaling, USA), anti-IRF3(1:100, Beyotime, China) followed by the secondary antibody (1:200, Beyotime,China). The nuclei were stained with DAPI. Finally, the fluorescence was detected using light microscopy and fluorescence microscopy. MRGECs were seeded onto circular coverslips and fixed with 4% formaldehyde for 10 min, followed by permeabilization with 0.1% Triton X-100 in PBS. The cells were blocked with 2% BSA at room temperature for 60 min and then incubated with primary anti-VE-cadherin(1:100, R&D systems Inc.,MN, USA), anti-NF-κB(1:100, Cell Signaling, USA), anti-IRF3(1:100, Beyotime, China) at 4°C overnight. Following incubation, samples were washed with PBS and incubated with secondary antibody. The coverslips were mounted using 90% glycerol in PBS, and the fluorescence was detected with light microscopy and fluorescence microscopy.

NO detection

The levels cellular NO were measured by a commercial NO assay kit (Beyotime, Haimen, China), according to the manufacturer's instructions. Briefly, the cells were lysed and centrifuged. RLU/OD was detected on 540nm by spectrum detection. The NO contents were calculated by constrast with the standard curve.

ROS detection

The levels of kidney and cellular ROS production were evaluated using standardized methods by ROS assay kit, according to the manufacturer's instructions(Beyotime, Haimen, China). Production of ROS was

evaluated by changes in the fluorescence intensity resulted from oxidation of the intracellular fluoroprobe 5- (and -6)-chloromethyl-2',7'-dichlorodihydrofluorescein diacetate (CM-H2DCF-DA, Molecular Probes, Eugene, OR, USA). ROS contents were observed or detected by confocal or fluorescence microscopy.

The measurement of blood urea and creatine.

Mice blood were collected before kidney harvest and kept at room temperature for 2 hours. Serum was isolated by 3500g for 10 minutes centrifugation. The serum was detected by ELISA blood urean and creatine assay kit(Westang Biotech, Shanghai,China) according to the manufacturer's instruction.

Doppler hemodynamics

The PeriCam PSI Zoom System was used to collect the blood flow perfusion data. Kidney blood flow was detected by PeriCam PSI Zoom 24 hours after CLP. The mice were anesthetized by isoflurane. Then kidneys were exposed and kidney blood flow was detected by PeriCam PSI Zoom.

Ca^{2+} image

Cytoplasmic calcium concentration was monitored using Zeiss 710 confocal confocal laser system. Briefly, cells were loaded with 10 mol/L Fluo-4/AM. Ca^{2+} stores was depleted by treating MRGEC with 4 mol/L thapsigargin for 6 to 8 minutes in a Ca^{2+}-free physiological saline ($0Ca^{2+}$-PSS), which contained (in mmol/L): 140 NaCl, 5 KCl, 1 $MgCl_2$, 10 glucose, 0.2 EGTA, 5 Hepes, pH 7.4. Ca^{2+} influx was initiated by applying1 mmol/L extracellular Ca2+. The cells were pretreated with/without HC for 1 hour before experiments. Changes in $[Ca^{2+}]_i$ were displayed as a ratio of fluorescence relative to the intensity before the application of extracellular Ca^{2+} (F1/F0).

siRNA transfection

siRNA and negative control were synthesized by GenePharma (Shanghai, China),siRNA sequences were as bellows: 5'-AAGACUUGUUCACGAAGAAAU-3'; 5'-UUCUUCGUGAACAAGUCUUUG-3'. siRNA transfection in vitro was performed by lipo8000(Beyotime, Shanghai, China), according to the manufactural instructions. The siRNA transfection in vivo was performed as follows: The TRPV4 siRNA or scrambled siRNA (5 mg/kg) was diluted in 50 uL of EntransterTM-in vivo RNA transfection reagent (Engreen Biosystem Co., Ltd., Beijing, China) and 10% glucose mixture according to the manufacturer's instructions. A volume of 50 uL siRNA or siTRPV4 mix was continuously subjected to mice by intravenous injection 3 days before CLP according to the reagent's instructions

Data analysis

All data are represented as mean ± SD. Statistical analysis between two groups was performed using student t test, and one-way ANOVA was used to compare the significance among three or more groups.

Bonferroni method was used to evaluate the significance conservatively. The calculations and data processing were performed using Sigmaplot 14.0.

Results

Blocking TRPV4 diminishes LPS-induced cytosolic Ca^{2+} -elevations.

Firstly, we measured whether LPS-induced Ca^{2+} entry was dependent on TRPV4. The MRGEC was stimulated by LPS after pretreated with HC or transfected with TRPV4siRNA. As expected, MRGEC pretreated with both HC and TRPV4siRNA displayed a significant reduction in LPS-induced cytosolic [Ca^{2+}] entry, relative to control group(Fig. 1a-f). As TLR4 recognizes LPS and drives the inflammatory response, which contributes to sepsis. Next, we reasoned that if other TLR ligand (TLR 1/2 ligand) induced Ca^{2+} entry was dependent on TRPV4. Consistent with these observation, a robust rise in cytosolic [Ca^{2+}] was observed after stimulation with CU-T12-9 (TLR 1/2 ligand) (10μM), but we failed to see the cytosolic [Ca^{2+}] reduction after treated by HC (Fig. 1g, h). Overall, these results clearly demonstrate that TRPV4 controls the Ca^{2+}-entry triggered by LPS. Considering that a Ca^{2+} entry mechanism involving store-operated Ca^{2+} entry (SOCE), and heteromeric TRPV4-C1 channels participate in mediating SOCE(22), we wondered that if blocking TRPV4 affects SOCE in MRGEC. In the next step, thapsigargin(TG) was used to delete Ca^{2+} store in endoplasmic reticulum, we found that inhibition of TRPV4 did not affect SOCE occurred(Fig. 1i, j).These results demonstrated that TRPV4 regulates the Ca^{2+}-entry triggered by LPS, but not the Ca^{2+}-entry triggered by CU-T12-9 or SOCE.

LPS-induced phosphorylation and translocation of NF-κB and IRF-3 is regulated by TRPV4.

LPS-initiated signaling triggers multiple post-translational modifications in the p65 subunit of NF-κB (NF-κB p65) (36). The phosphorylation of NF-κB p65 is associated with nuclear translocation(42) and transcriptional transactivation(40), respectively. Likewise, phosphorylation at IRF3 is crucial for the induction of Type I IFNs(19). Next, we examined if LPS-induced phosphorylation of either NF-κB p65 or IRF3 was impaired after inhibition or knockdown of TRPV4. LPS stimulation (1μg/ml) induced the phosphorylation and translocation of NF-κB and IRF-3, and this effect was significantly decreased compared to HC treatment or TRPV4 transfection((Fig. 2. g, h, j, k, l, n). As a proximal readout, degradation of IκBα may indicate the degree of signal transduction upstream of NF-κB p65. We also measured the degradation of IκBα, we did not observe significant change in IκBα protein levels after HC treatment or TRPV4siRNA transfection, suggesting that TRPV4 regulates LPS signaling downstream of IκBα(Fig. 2. g, i, k, m). Thus, in the absence of TRPV4, LPS-induced phosphorylation of the key transcription factors, NF-κB and IRF-3 are significantly compromised.

TRPV4 inhibition reduced glomerular endothelial inflammation and enhanced endothelial cell barrier function.

To determine if inhibition of TRPV4 attenuated LPS-induced endothelial inflammation, MRGEC was pretreated with HC before stimulated by LPS. Our data showed that LPS caused significant increase of endothelial adhesion molecules including VCAM1, ICAM1 and E-selectin, which was inhibited by HC treatment(Fig. 3a, b). Next, phalloidin and VE-cadherin were stained to assess cytoskeletal remodeling and adherens junction integrity in endothelial cells, respectively. These results showed that LPS induced massive formation of actin stress fibers and intercellular gaps due to cell contractions in MRGEC. These changes were largely reduced by HC treatment (Fig. 3c). During sepsis, the production of ROS injures the endothelium and damages extracellular structures such as cell membranes and glycocalyx directly. In addition, it also can impair the endothelium-dependent vasoreactivity(4).The DCFH-DA detection showed that LPS increases ROS production strongly, which was suppressed by HC treatment(Fig. 3d).It is general accept that the NO system is a major contributor to endothelial injury, thus we detected the expression of eNOS in the next step. It can be seen clearly that LPS significant decreased phosphorylation of eNOS, while HC treatment did not increase the level of p-eNOS as well was the production of NO(Fig. 3e-g),suggesting that TRPV4 inhibition reduced glomerular endothelial inflammation and enhanced cell barrier function without altering the NO production.

Clamping intracellular Ca^{2+} mimics the defects in LPS response seen in the absence of TRPV4.

It is reported that stimulation of the T cell receptor (TCR), but not tumor necrosis factor receptor (TNFR), induces a Ca^{2+}-dependent phosphorylation of NF-κB p65 (20). It is, however, unknown if LPS-induced phosphorylation of NF-κB p65 requires intracellular Ca^{2+} or $[Ca^{2+}]_i$ elevations in MRGEC. We depleted and clamped $[Ca^{2+}]_i$ by loading MRGEC with the high affinity membrane permeable Ca^{2+}-chelator BAPTA-AM and then stimulated them with LPS. Preventing $[Ca^{2+}]_i$ elevations decreased the phosphorylation and translocation of NF-κB p65 induced by LPS stimulation (Fig. 4a-c). We then measured whether LPS-induced increase of endothelial adhesion molecules was diminished by clamping intracellular Ca^{2+}. We found that loading MRGEC with BAPTA-AM caused decrease of VCAM1, ICAM1 and E-selectin(Fig. 4d,e). As we verified before that Ca^{2+}-entry triggered by CU-T12-9 was not dependent on TRPV4, we want to investigate whether TRPV4 participates in CU-T12-9-induced endothelial inflammation. Consistent with previous results, our data showed that CU-T12-9 inhibition of TRPV4 has no significant impact on CU-T12-9-induced endothelial inflammation(Fig. 4.f-h).

Inhibition of TRPV4 reduced glomerular endothelial inflammation and retained translocation of NF-κB and IRF-3 in CLP-induced sepsis.

To further investigate whether TRPV4 contribute to glomerular endothelial inflammation in vivo, HC(11, 33), the highly selective inhibitors which have been shown to be well tolerated in vivo with minimal side effects was used(35). We employed the widely used polymicrobial sepsis model, CLP. As showed in Fig. 5a-d, glomerulus of mice pretreated with HC showed lower expression of VCAM1 and E-selectin than CLP-operated mice. Consistent with this, mice with HC treatment exhibited significantly reduced levels of CD68 positive macrophages infiltration into the endothelium (Fig. 5e). As we have demonstrated that

TRPV4 regulated LPS-induced translocation of NF-κB and IRF-3 in MGREC, in the next we detected the distribution of NF-κB and IRF-3 in glomerulus of mice. Our data showed that mice after CLP operated exhibited increased translocation of NF-κB and IRF-3, which was repressed by HC treatment(Fig. 5f,g). These results suggested that of TRPV4 mitigated glomerular endothelial inflammation possibly through inhibition of NF-κB and IRF-3 and their signal transduction downsteam.

Inhibition or knockdown of TRPV4 ameliorates CLP-induced kidney injury and renal function.

To evaluate the role of TRPV4 in sepsis, HE staining was performed to observe the extent of kidney injury. Our results revealed that 24 hours after CLP caused greater inflammatory cell infiltration in the glomeruli and tubulointerstitium, tubular epithelial cells swell and vacuolation, cast formation in the tubules, and glomerulus atrophy in the kidneys compared with those in sham-operated WT mice (Fig. 6a). However, mice administrated with HC or exhibited much weaker renal damage and much lower Jablonski Grade scores than those of CLP-operated mice (Fig. 6b). As renal hypoperfusion is one of the main characteristics of S-AKI, we wondered that whether TRPV4 inhibition improves CLP-induced renal hypoperfusion. Color doppler flow imaging was used to detect local renal blood flow, our result showed that 24 hours after mice received CLP operation exhibited significant reduction of renal perfusion(Fig. Supplemental). TRPV4 inhibition did not improve renal hypoperfusion(Fig. 6d, e), which was contrary to our previous study(10). Mice subjected to CLP died within 3 days, with a survival rate of 43% after 24 hours. In contrast, the 24-hour survival rate of mice that received HC, 1 hour prior to the CLP surgery was 85% (Fig. 6c). To further verify the protective effect of TRPV4 inhibition in sepsis, we applied siRNA interference to downregulate TRPV4 in vivo. Mice were received the NCsiRNA or TRPV4 siRNA 3 days prior to the CLP surgery.24 hours after subjected to CLP, HE staining revealed that knockdown of TRPV4 ameliorates renal damage and exhibited much lower Jablonski Grade scores than those of CLP-operated mice pretreated with NCsiRNA(Fig. 6f, g). The survival rate of NCsiRNA treated mice was 37.5% and that of 75% of TRPV4siRNA transfection(Fig. 6h). However, local renal blood flow was not affected after knockdown of TRPV4 as showed in Fig. 6.k,l. Furthermore, we measured the serum levels of BUN and creatinine to functionally identify the renoprotective effect of TRPV4 knockdown in mice with CLP. Mice with CLP-operated after NCsiRNA-pretreated showed significant increased levels of BUN(Fig. 6i) and creatinine (Fig. 6j), while TRPV4 knockdown strongly alleviated these effects.

Discussion

In the present study, we have uncovered a novel TRPV4-mediated Ca^{2+}-signaling pathway that is essential for LPS-induced glomerular endothelial inflammation and S-AKI and is, therefore, critical to innate immunity. TRPV4 mediates cytosolic Ca^{2+} elevations in response to LPS, and this Ca^{2+} influx is necessary for glomerular endothelial cells activation. An important reason for this phenomenon is the Ca^{2+}-influx also regulates the activation and nuclear translocation of NF-κB and IRF-3. Thus, TRPV4 controls the transcriptional programs mediated by these key transcription factors during CLP-induced sepsis associated AKI.

The role of TRPV4 in ECs under endotoxin stimulation has been demonstrated previously(23). The mechanism involving in glomerular endothelial function and inflammation induced by sepsis has remained elusive. Firstly, we investigated whether TRPV4 suppression significantly attenuated the increase in $[Ca^{2+}]_i$ induced by the LPS, as expected, treatment with HC or transfected with TRPV4siRNA prevented LPS-induced cytosolic $[Ca^{2+}]_i$ elevations(Fig. 1a-f). To examine whether TRPV4 was required for signaling through other TLRs, we stimulated MGREC with CU-T12-9, which is TLR1/2 agonist and measured whether CU-T12-9 induced Ca^{2+} entry was dependent on TRPV4. We found that MGREC stimulated with CU-T12-9 displayed a significant increase of cytosolic $[Ca^{2+}]$ entry, relative to control group. However, CU-T12-9-induced Ca^{2+} entry occurred independently of TRPV4(Fig. 1g, h). It is documented that heteromeric TRPV4-TRPC1 channels contribute to SOCE in vascular endothelial cells(22).TRPV4 associated with Ca^{2+}-activated potassium channels contribute to modulating SOCE with physiological relevance(27). Furthermore, endothelial cells, which fail to trigger SOCE limits LPS-induced vascular inflammation(14). Based on these, we wondered whether inhibition of TRPV4 affect the response of SOCE in MRGEC. Our results showed that blocking TRPV4 did not affect SOCE (Fig. 1i-j), indicating that TRPV4 mainly participates in TLR4 signaling, mediates intracellular Ca^{2+} overload without altering SOCE.

Remarkably, a thorough study demonstrated that inhibition of the NF-κB in choroid plexus epithelial cells, involved in the production and regulation of several inflammatory cytokines, inhibited TRPV4-mediated activity, suggesting a link between TRPV4 and cytokine production(31). However, another study reported that TRPV4 is dispensable for LPS-induced nuclear translocation of NF-κB in in urothelial cells. (2). According to these previous study, in our next study, we found that TRPV4 participates in LPS-induced phosphorylation and tranlocation of NF-κB and IRF3in MRGEC. Inhibition or knockdown of TRPV4 repressed the activation of NF-κb and IRF3(Fig. 2e-g,h,j,k,l,n). Interestingly, IκBα degradation appears to be unaffected after inhibition or knockdown of TRPV4 in MRGEC(Fig. 2g,i,k,m). This observation suggests that TRPV4-dependent Ca^{2+}-signaling can greatly modify NF-κB signaling from different aspects. The local Ca^{2+}-influx promotes the TLR4 signaling which is critical to downstream signaling, including IRF-3 activation.

In the skin, TRPV4 contributes to the development and maturation of cell-cell junctions in epithelia of the skin(32). It directly interacts with β-catenin and E-cadherin, thereby results in strengthened cell-cell adhesion structures between keratinocytes and the basal membrane(21, 32), thus forming a physical barrier against external environmental insults. Of note, TRPV4 is prominently expressed in endothelial cells, where it is involved in the hyper-inflammatory response and mortality associated with sepsis(9). In the next study, we wondered whether TRPV4 play a critical role in LPS-induced cell-cell junction disruption and production of endothelial adhesion molecules. Our results demonstrated that LPS stimulation caused an increase in VCAM1, ICAM1 and E-selectin, which were reduced by HC treatment(Fig. 3a, b).This fall in line with previous study that higher plasma levels of E-selectin and/or ICAM-1 correlate with damage of organs, severity of sepsis, and mortality(16, 30).And a decrease in ICAM-1 and E-selectin expression correlates with decreased neutrophil infiltration in lung, liver and kidney and a decrease in

tissue damage(41). Inhibition of TRPV4 also enhanced endothelial cell barrier function as observed in immunofluorescence (Fig. 3c), indicating that TRPV4 is excessive activated during sepsis, thus promotes intercellular permeability. What we should consider is, a recent and comprehensive study demonstrated that TRPC6 deficiency prevented lung endothelial hyperpermeability, and reduced mortality up to 70% after LPS challenge(34). While pointing to a different TRP channel, these observations may be complementary with our results. Accordingly, inhibition of TRPV4 reduced the LPS-induced ROS production (Fig. 3d).These observation provided a strong envidence that TRPV4 participates in mediating kidney injury during an inflammatory systemic insult. It is reported that TRPV4-mediated rise in Ca^{2+} induces the activation of nitric oxide synthases (eNOS and iNOS) expressed in epithelial cells, increasing NO production in the luminal compartment, resulting in a bactericidal effect(6). On the other hand, NO would decrease leukocyte adhesion to endothelial cells through down-regulation of cell adhesion molecules (8, 17). Thus we detected whether inhibition of TRPV4 affects the expression of eNOS and the production of NO. As can be seen from Fig. 3e-f, HC treatment did not increase the level of p-eNOS as well was the production of NO, suggesting that TRPV4 inhibition alleviated glomerular endothelial injury without improving the NO decrease.

Acute kidney injury is a frequent and serious complication during sepsis. To better understand the nature of LPS-induced $[Ca^{2+}]_i$ mobilization, MRGEC were loaded with BAPTA-AM and then stimulated with LPS, BAPTA-AM-loaded cells showed a drastic reduction of VCAM1, ICAM1 and E-selectin as well as the p-NF-κB and p-IRF-3 (Fig. 4a,c-e).The nuclear translocation of NF-κB was also prevented after diminishing cytosolic $[Ca^{2+}]_i$ elevations(Fig. 4b), confirming that Ca^{2+}-signaling is essential for LPS-induced response.

To further investigate whether TRPV4 is critical to glomerular endothelial inflammation in vivo, we used a specific TRPV4 antagonist, HC, and found that TRPV4 inhibition reduced CLP-induced increase of VCAM1, E-selectin in glomerulis of mice(Fig. 5a-d). Accordingly, mice with HC treatment exhibited significant reduced levels of CD68 positive macrophages infiltration into the endothelium in glomeruli(Fig. 5e). Furthermore, the translocation of NF-κB and IRF-3 glomeruli was also depressed by HC treatment(Fig. 5f,g).

As these observation, we wondered whether inhibition of TRPV4 ameliorate AKI in sepsis, HC was used to block TRPV4 and we found that TRPV4 inhibition ameliorates CLP-induced kidney injury (Fig. 6a,b).We also detected the renal blood flow after inhibiting TRPV4, surprisingly, our result showed that TRPV4 inhibition did not improve renal hypoperfusion(Fig. 1d, e),indicating that the protective effect of TRPV4 inhibition on S-AKI was not dependent on renal hypoperfusion. Besides, the 24-hour survival rate of mice that received HC was improved(Fig. 6c). Next, we applied specific siRNA targeting TRPV4 to downregulate TRPV4 expression and investigated whether TRPV4 is involved in CLP-induced AKI. Our results showed that mice administrated with TRPV4siRNA decreased tubulointerstitial damage, renal dysfunction, serum level of BUN and CRE(Fig. 6f,g,i,j). The survival rate of mice was also increased, which is congruent with the effect of HC(Fig. 6h). However, the local renal blood flow after CLP was still unaffected by TRPV4siRNA administration(Fig. 6k, l). In our view, there may be a variety of mechanisms involving in

regulating local renal blood flow, alterations of renal blood flow after sepsis are due to insufficient hemodynamic optimization or specific microvascular injuries induced by sepsis (endothelial dysfunction, increased leukocyte adhesion, rheological abnormalities, glycocalyx alterations and functional shunting) (15). Consistent with our study, previous study reported that TLR4 inhibitor is able to reverse a manifest impairment in renal function caused by sepsis, but it does not involve in improving macro-circulation or micro-circulation, enhancing renal oxygen delivery, or attenuating tubular necrosis(13). Thus, our in vivo experimental results revealed that inhibition or knockdown of TRPV4 exerted a protective effect of CLP-induced AKI without improving local renal blood flow. However, the deep molecular mechanism of TRPV4 involving in S-AKI injury needs to be defined.

Conclusion

Overall, in this study, we provide the first evidence that inhibition of TRPV4 ameliorates glomerular endothelial inflammation, kidney dysfunction, and increased mortality via mediating Ca^{2+} overload and NF-κB/IRF-3 activation under sepsis situation. Therefore, from a clinical perspective, it should be carefully considered the application of TRPV4 antagonists as a treatment option in the future.

Declarations

Availability of data and materials

All data generated or analyzed in this study are included in this published article and its supplementary information files.

Ethics approval and consent to participate

Animals were handled in accordance with procedures approved by Medical Ethics Committee of Shanghai Jiaotong University, and were performed in strict accordance with approved guidelines.

Consent for publication

Not applicable.

Competing interests

The authors declare that they have no conflict of interest.

Funding

This study was supported by National Natural Science Foundation of China (81830010, 81330006 and 81900438)；grant from Science and Technology Commission of Shanghai Municipality (18411950400).

Authors' contributions

Ben He and Linghong Shen participated in the research design and revised the manuscript; XW performed the experiments and paper writing; YHW performed the western blot and animal model establishment; Guo Zhou and Yi Li helped with the animal experiment and siRNA transfection; Feng Liang, Jieyuan Xue, Xin Shi, Anwen Yin and Qingqing Xiao assisted with experiments and analyzed data.

Acknowledgements

Not applicable.

Authors' information

[1]Department of Cardiology, Shanghai Chest Hospital, Shanghai Jiaotong University, Shanghai, China, 200030

[2]Department of critical medicine, Shanghai Chest Hospital, Shanghai Jiaotong University, Shanghai, China, 200030

References

1. Alpizar Y.A., Boonen B., Sanchez A., Jung C., Lopez-Requena A., Naert R., Steelant B., Luyts K., Plata C., De Vooght V., Vanoirbeek J., Meseguer V.M., Voets T., Alvarez J.L., Hellings P.W., Hoet P., Nemery B., Valverde M.A. and Talavera K. TRPV4 activation triggers protective responses to bacterial lipopolysaccharides in airway epithelial cells. NAT COMMUN 8(1):1059, 2017.
2. Alpizar Y.A., Uvin P., Naert R., Franken J., Pinto S., Sanchez A., Gevaert T., Everaerts W., Voets T., De Ridder D. and Talavera K. TRPV4 Mediates Acute Bladder Responses to Bacterial Lipopolysaccharides. FRONT IMMUNOL 11:799, 2020.
3. Alvarez D.F., King J.A., Weber D., Addison E., Liedtke W. and Townsley M.I. Transient receptor potential vanilloid 4-mediated disruption of the alveolar septal barrier: a novel mechanism of acute lung injury. CIRC RES 99(9):988–995, 2006.
4. Araujo M. and Welch W.J. Oxidative stress and nitric oxide in kidney function. Curr Opin Nephrol Hypertens 15(1):72–77, 2006.
5. Balakrishna S., Song W., Achanta S., Doran S.F., Liu B., Kaelberer M.M., Yu Z., Sui A., Cheung M., Leishman E., Eidam H.S., Ye G., Willette R.N., Thorneloe K.S., Bradshaw H.B., Matalon S. and Jordt S.E. TRPV4 inhibition counteracts edema and inflammation and improves pulmonary function and oxygen saturation in chemically induced acute lung injury. Am J Physiol Lung Cell Mol Physiol 307(2):L158-L172, 2014.
6. Boonen B., Alpizar Y.A., Meseguer V.M. and Talavera K. TRP Channels as Sensors of Bacterial Endotoxins. Toxins (Basel) 10(8), 2018.
7. Brooks C., Wei Q., Cho S.G. and Dong Z. Regulation of mitochondrial dynamics in acute kidney injury in cell culture and rodent models. J CLIN INVEST 119(5):1275–1285, 2009.

8. Dal Secco D., Paron J.A., de Oliveira S.H., Ferreira S.H., Silva J.S. and Cunha F.Q. Neutrophil migration in inflammation: nitric oxide inhibits rolling, adhesion and induces apoptosis. Nitric Oxide 9(3):153–164, 2003.
9. Dalsgaard T., Sonkusare S.K., Teuscher C., Poynter M.E. and Nelson M.T. Pharmacological inhibitors of TRPV4 channels reduce cytokine production, restore endothelial function and increase survival in septic mice. Sci Rep 6:33841, 2016.
10. Du J, Wang X., Li J., Guo J., Liu L., Yan D., Yang Y., Li Z., Zhu J. and Shen B. Increasing TRPV4 expression restores flow-induced dilation impaired in mesenteric arteries with aging. Sci Rep 6:22780, 2016.
11. Everaerts W., Zhen X., Ghosh D., Vriens J., Gevaert T., Gilbert J.P., Hayward N.J., McNamara C.R., Xue F., Moran M.M., Strassmaier T., Uykal E., Owsianik G., Vennekens R., De Ridder D., Nilius B., Fanger C.M. and Voets T. Inhibition of the cation channel TRPV4 improves bladder function in mice and rats with cyclophosphamide-induced cystitis. Proc Natl Acad Sci U S A 107(44):19084–19089, 2010.
12. Fani F., Regolisti G., Delsante M., Cantaluppi V., Castellano G., Gesualdo L., Villa G. and Fiaccadori E. Recent advances in the pathogenetic mechanisms of sepsis-associated acute kidney injury. J NEPHROL 31(3):351–359, 2018.
13. Fenhammar J., Rundgren M., Hultenby K., Forestier J., Taavo M., Kenne E., Weitzberg E., Eriksson S., Ozenci V., Wernerson A. and Frithiof R. Renal effects of treatment with a TLR4 inhibitor in conscious septic sheep. CRIT CARE 18(5):488, 2014.
14. Gandhirajan R.K., Meng S., Chandramoorthy H.C., Mallilankaraman K., Mancarella S., Gao H., Razmpour R., Yang X.F., Houser S.R., Chen J., Koch W.J., Wang H., Soboloff J., Gill D.L. and Madesh M. Blockade of NOX2 and STIM1 signaling limits lipopolysaccharide-induced vascular inflammation. J CLIN INVEST 123(2):887–902, 2013.
15. Harrois A., Grillot N., Figueiredo S. and Duranteau J. Acute kidney injury is associated with a decrease in cortical renal perfusion during septic shock. CRIT CARE 22(1):161, 2018.
16. Kayal S., Jais J.P., Aguini N., Chaudiere J. and Labrousse J. Elevated circulating E-selectin, intercellular adhesion molecule 1, and von Willebrand factor in patients with severe infection. Am J Respir Crit Care Med 157(3 Pt 1):776–784, 1998.
17. Kosonen O., Kankaanranta H., Malo-Ranta U. and Moilanen E. Nitric oxide-releasing compounds inhibit neutrophil adhesion to endothelial cells. EUR J PHARMACOL 382(2):111–117, 1999.
18. Liedtke W., Choe Y., Marti-Renom M.A., Bell A.M., Denis C.S., Sali A., Hudspeth A.J., Friedman J.M. and Heller S. Vanilloid receptor-related osmotically activated channel (VR-OAC), a candidate vertebrate osmoreceptor. CELL 103(3):525–535, 2000.
19. Lin R., Mamane Y. and Hiscott J. Structural and functional analysis of interferon regulatory factor 3: localization of the transactivation and autoinhibitory domains. MOL CELL BIOL 19(4):2465–2474, 1999.
20. Liu X., Berry C.T., Ruthel G., Madara J.J., MacGillivray K., Gray C.M., Madge L.A., McCorkell K.A., Beiting D.P., Hershberg U., May M.J. and Freedman B.D. T Cell Receptor-induced Nuclear Factor

kappaB (NF-kappaB) Signaling and Transcriptional Activation Are Regulated by STIM1- and Orai1-mediated Calcium Entry. J BIOL CHEM 291(16):8440–8452, 2016.

21. Lu Q., Zemskov E.A., Sun X., Wang H., Yegambaram M., Wu X., Garcia-Flores A., Song S., Tang H., Kangath A., Cabanillas G.Z., Yuan J.X., Wang T., Fineman J.R. and Black S.M. Activation of the mechanosensitive Ca(2+) channel TRPV4 induces endothelial barrier permeability via the disruption of mitochondrial bioenergetics. REDOX BIOL 38:101785, 2021.
22. Ma X., Cheng K.T., Wong C.O., O'Neil R.G., Birnbaumer L., Ambudkar I.S. and Yao X. Heteromeric TRPV4-C1 channels contribute to store-operated Ca(2+) entry in vascular endothelial cells. CELL CALCIUM 50(6):502–509, 2011.
23. Maier-Begandt D., Comstra H.S., Molina S.A., Kruger N., Ruddiman C.A., Chen Y.L., Chen X., Biwer L.A., Johnstone S.R., Lohman A.W., Good M.E., DeLalio L.J., Hong K., Bacon H.M., Yan Z., Sonkusare S.K., Koval M. and Isakson B.E. A venous-specific purinergic signaling cascade initiated by Pannexin 1 regulates TNFalpha-induced increases in endothelial permeability. SCI SIGNAL 14(672), 2021.
24. Mehta R.L., Kellum J.A., Shah S.V., Molitoris B.A., Ronco C., Warnock D.G. and Levin A. Acute Kidney Injury Network: report of an initiative to improve outcomes in acute kidney injury. CRIT CARE 11(2):R31, 2007.
25. Moran M.M., McAlexander M.A., Biro T. and Szallasi A. Transient receptor potential channels as therapeutic targets. NAT REV DRUG DISCOV 10(8):601–620, 2011.
26. Obeidat M., Obeidat M. and Ballermann B.J. Glomerular endothelium: a porous sieve and formidable barrier. EXP CELL RES 318(9):964–972, 2012.
27. Pizzoni A., Lopez G.M., Di Giusto G., Rivarola V., Capurro C. and Ford P. AQP2 can modulate the pattern of Ca(2+) transients induced by store-operated Ca(2+) entry under TRPV4 activation. J CELL BIOCHEM 119(5):4120–4133, 2018.
28. Rhodes A., Evans L.E., Alhazzani W., Levy M.M., Antonelli M., Ferrer R., Kumar A., Sevransky J.E., Sprung C.L., Nunnally M.E., Rochwerg B., Rubenfeld G.D., Angus D.C., Annane D., Beale R.J., Bellinghan G.J., Bernard G.R., Chiche J.D., Coopersmith C., De Backer D.P., French C.J., Fujishima S., Gerlach H., Hidalgo J.L., Hollenberg S.M., Jones A.E., Karnad D.R., Kleinpell R.M., Koh Y., Lisboa T.C., Machado F.R., Marini J.J., Marshall J.C., Mazuski J.E., McIntyre L.A., McLean A.S., Mehta S., Moreno R.P., Myburgh J., Navalesi P., Nishida O., Osborn T.M., Perner A., Plunkett C.M., Ranieri M., Schorr C.A., Seckel M.A., Seymour C.W., Shieh L., Shukri K.A., Simpson S.Q., Singer M., Thompson B.T., Townsend S.R., Van der Poll T., Vincent J.L., Wiersinga W.J., Zimmerman J.L. and Dellinger R.P. Surviving Sepsis Campaign: International Guidelines for Management of Sepsis and Septic Shock: 2016. CRIT CARE MED 45(3):486-552, 2017.
29. Ricci Z. and Ronco C. Pathogenesis of acute kidney injury during sepsis. CURR DRUG TARGETS 10(12):1179–1183, 2009.
30. Sessler C.N., Windsor A.C., Schwartz M., Watson L., Fisher B.J., Sugerman H.J. and Fowler A.R. Circulating ICAM-1 is increased in septic shock. Am J Respir Crit Care Med 151(5):1420–1427, 1995.

31. Simpson S., Preston D., Schwerk C., Schroten H. and Blazer-Yost B. Cytokine and inflammatory mediator effects on TRPV4 function in choroid plexus epithelial cells. Am J Physiol Cell Physiol 317(5):C881-C893, 2019.
32. Sokabe T., Fukumi-Tominaga T., Yonemura S., Mizuno A. and Tominaga M. The TRPV4 channel contributes to intercellular junction formation in keratinocytes. J BIOL CHEM 285(24):18749–18758, 2010.
33. Sonkusare S.K., Bonev A.D., Ledoux J., Liedtke W., Kotlikoff M.I., Heppner T.J., Hill-Eubanks D.C. and Nelson M.T. Elementary Ca2+ signals through endothelial TRPV4 channels regulate vascular function. SCIENCE 336(6081):597–601, 2012.
34. Tauseef M., Knezevic N., Chava K.R., Smith M., Sukriti S., Gianaris N., Obukhov A.G., Vogel S.M., Schraufnagel D.E., Dietrich A., Birnbaumer L., Malik A.B. and Mehta D. TLR4 activation of TRPC6-dependent calcium signaling mediates endotoxin-induced lung vascular permeability and inflammation. J EXP MED 209(11):1953–1968, 2012.
35. Thorneloe K.S., Cheung M., Bao W., Alsaid H., Lenhard S., Jian M.Y., Costell M., Maniscalco-Hauk K., Krawiec J.A., Olzinski A., Gordon E., Lozinskaya I., Elefante L., Qin P., Matasic D.S., James C., Tunstead J., Donovan B., Kallal L., Waszkiewicz A., Vaidya K., Davenport E.A., Larkin J., Burgert M., Casillas L.N., Marquis R.W., Ye G., Eidam H.S., Goodman K.B., Toomey J.R., Roethke T.J., Jucker B.M., Schnackenberg C.G., Townsley M.I., Lepore J.J. and Willette R.N. An orally active TRPV4 channel blocker prevents and resolves pulmonary edema induced by heart failure. SCI TRANSL MED 4(159):148r-159r, 2012.
36. Vallabhapurapu S. and Karin M. Regulation and function of NF-kappaB transcription factors in the immune system. ANNU REV IMMUNOL 27:693–733, 2009.
37. Verma S.K. and Molitoris B.A. Renal endothelial injury and microvascular dysfunction in acute kidney injury. SEMIN NEPHROL 35(1):96–107, 2015.
38. Vriens J., Watanabe H., Janssens A., Droogmans G., Voets T. and Nilius B. Cell swelling, heat, and chemical agonists use distinct pathways for the activation of the cation channel TRPV4. Proc Natl Acad Sci U S A 101(1):396–401, 2004.
39. Watanabe H., Vriens J., Prenen J., Droogmans G., Voets T. and Nilius B. Anandamide and arachidonic acid use epoxyeicosatrienoic acids to activate TRPV4 channels. NATURE 424(6947):434–438, 2003.
40. Yang F., Tang E., Guan K. and Wang C.Y. IKK beta plays an essential role in the phosphorylation of RelA/p65 on serine 536 induced by lipopolysaccharide. J IMMUNOL 170(11):5630–5635, 2003.
41. Ye X., Ding J., Zhou X., Chen G. and Liu S.F. Divergent roles of endothelial NF-kappaB in multiple organ injury and bacterial clearance in mouse models of sepsis. J EXP MED 205(6):1303–1315, 2008.
42. Zhong H., SuYang H., Erdjument-Bromage H., Tempst P. and Ghosh S. The transcriptional activity of NF-kappaB is regulated by the IkappaB-associated PKAc subunit through a cyclic AMP-independent mechanism. CELL 89(3):413–424, 1997.

Figures

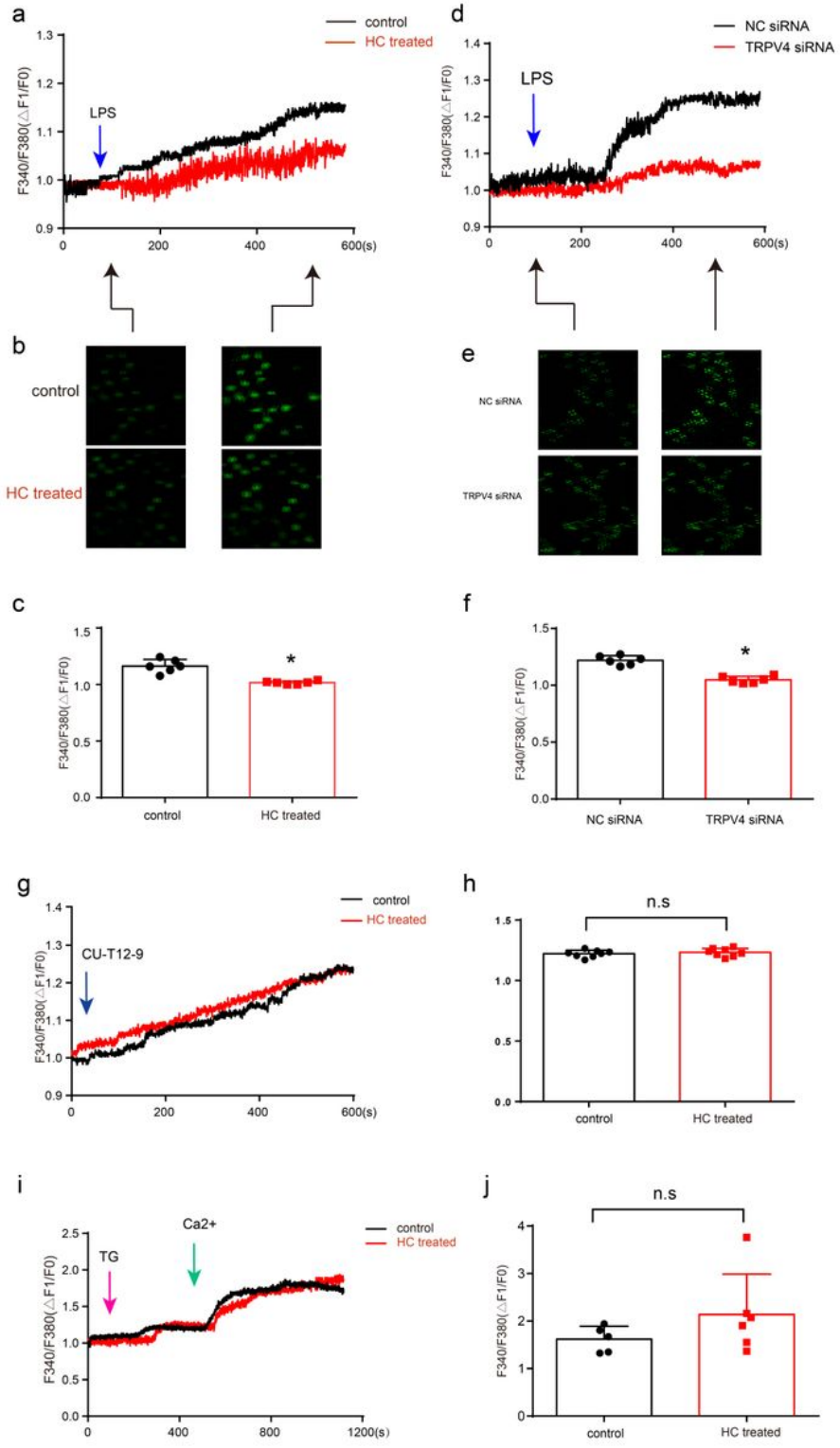

Figure 1

LPS-induced Ca2+ elevations are highly compromised in TRPV4-deficient MGREC. a Relative changes in [Ca2+]i over time in DMSO and HC pretreated cells for 10 min. Cells were treated with LPS (1μg/ml). b. Representative fluorescence images from indicated time points in the experiments shown in panel a. c.

Statistical representation of mean peak intensities of Fluo-4 fluorescence after LPS treatment. *P < 0.05, n = 6. d. Relative changes in [Ca2+]i over time in DMSO and TRPV4siRNA transfected cells for 10 min. Cells were treated with LPS (1μg/ml). e. Representative fluorescence images from indicated time points in the experiments shown in panel d. g. Relative changes in [Ca2+]i over time in DMSO and CU-T12-9 pretreated cells for 10 min. Cells were treated with LPS (1μg/ml). h. Statistical representation of mean peak intensities of Fluo-4 fluorescence after LPS treatment. *P < 0.05, n = 6.i. Relative changes in [Ca2+]i over time after deleted Ca2+ store with TG(1μM) and then treated with Ca2+(2mM).j. Statistical representation of mean peak intensities of Fluo-4 fluorescence after TG and Ca2+ treatment. *P < 0.05, n = 6.

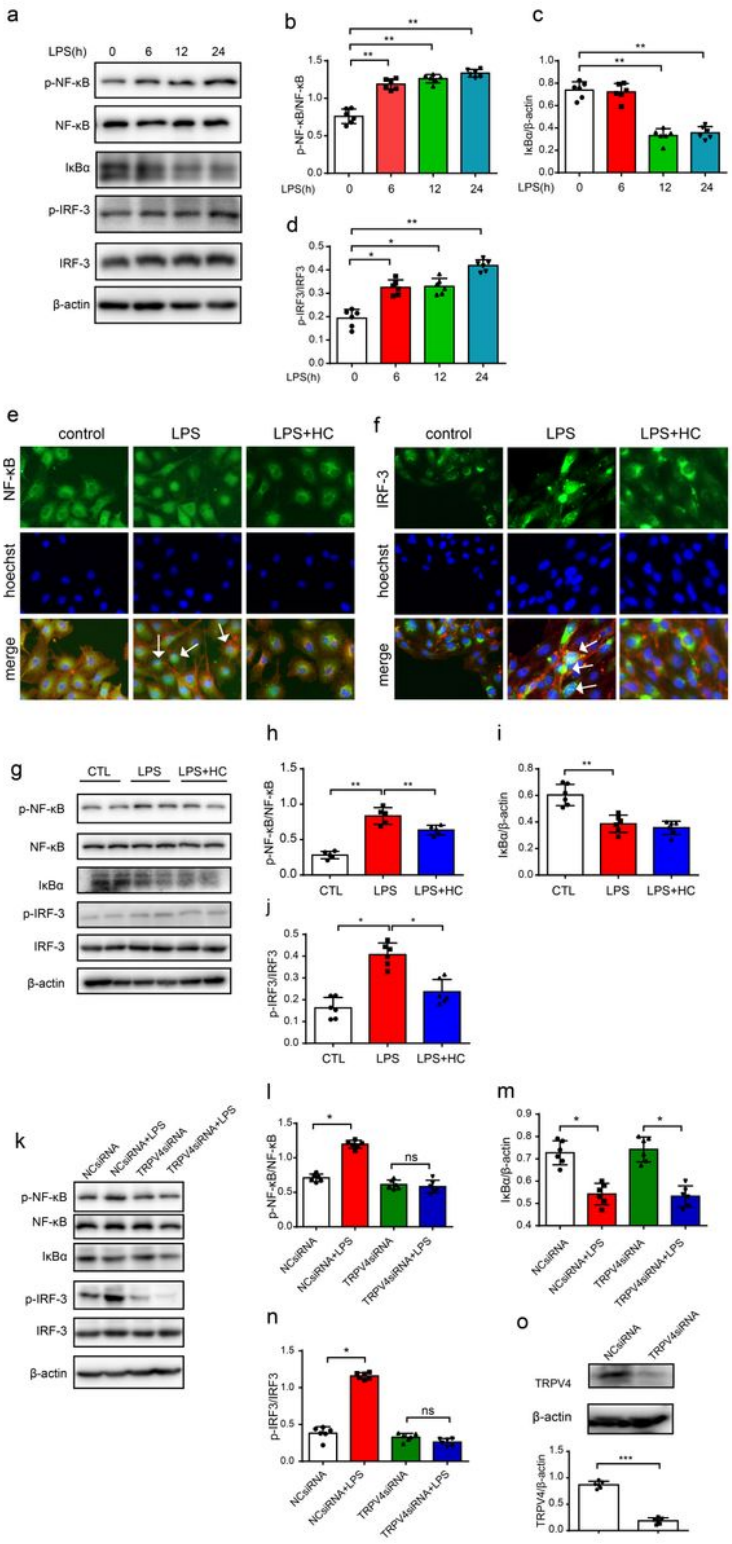

Figure 2

TRPV4 mediates LPS-induced phosphorylation and tranlocation of NF-κB. a- d. The expression of p-NF-κB p65, NF-κB p65, iκBα, p-IRF-3 and IRF-3 was analyzed by western blot. Cells were stimulated with LPS (1μg/mL) as indicated. Densitometry values indicate phospho-protein levels relative to total protein (ratios). **P < 0.01, n = 6.e-f. Immunofluorescence staining of NF-κB and IRF-3 was performed. Quantification of nuclear translocation is reflected by and directly proportional to the similarity scores of

NF-κB or IRF-3 and nuclear staining. Original magnification, ×200. g-j. The protein level of p-NF-κB p65, NF-κB p65, iκBα, p-IRF-3 and IRF-3 was analyzed by western blot. Cells were stimulated by LPS (1μg/mL) with or without HC. **P < 0.01, n = 6. k-n. The protein level of p-NF-κB p65, NF-κB p65, iκBα, p-IRF-3 and IRF-3 was analyzed by western blot. Cells were stimulated by LPS (1μg/mL) with TRPV4siRNA or NCsiRNA transfection. *P < 0.05, ***P < 0.001, n = 6.o. The protein level of TRPV4 was analyzed by western blot. Cells were transfected by TRPV4siRNA. ***P < 0.001, n = 6.

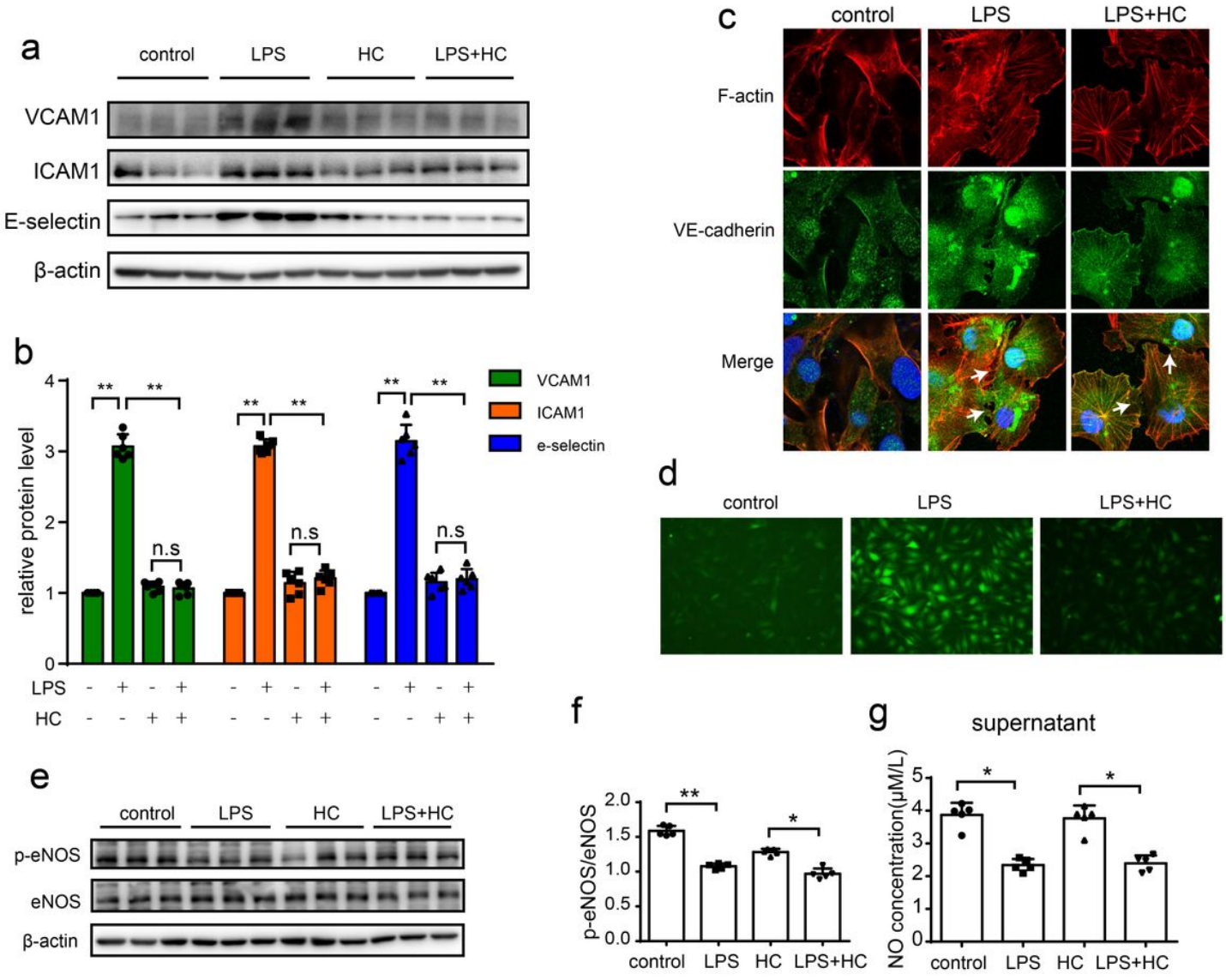

Figure 3

TRPV4 inhibition reduced the expression of endothelial adhesion molecules and enhanced endothelial cell barrier function. MGREC were treated with 1 μM HC 1 hour before 1 μg/mL LPS administration. a, b. The protein level of VCAM1, ICAM1 and E-selectin was determined by western blot. **P < 0.01, n = 6.c. Phalloidin and VE-cadherin staining for assessing cytoskeletal remodeling and adherens junction integrity in MRGEC 24 hours after LPS and HC treatment. magnification, ×200. Arrows in the Phalloidin and VE-cadherin staining represent gaps between the cells. d. The DCFH-DA staining showed the production of ROS. magnification, ×50. e, f. The protein level of p-eNOS and eNOS was determined by

western blot. *P < 0.05, **P < 0.01, n = 6. g. The NO production in supernatant was detected by NO assay kit. *P < 0.05, n = 6.

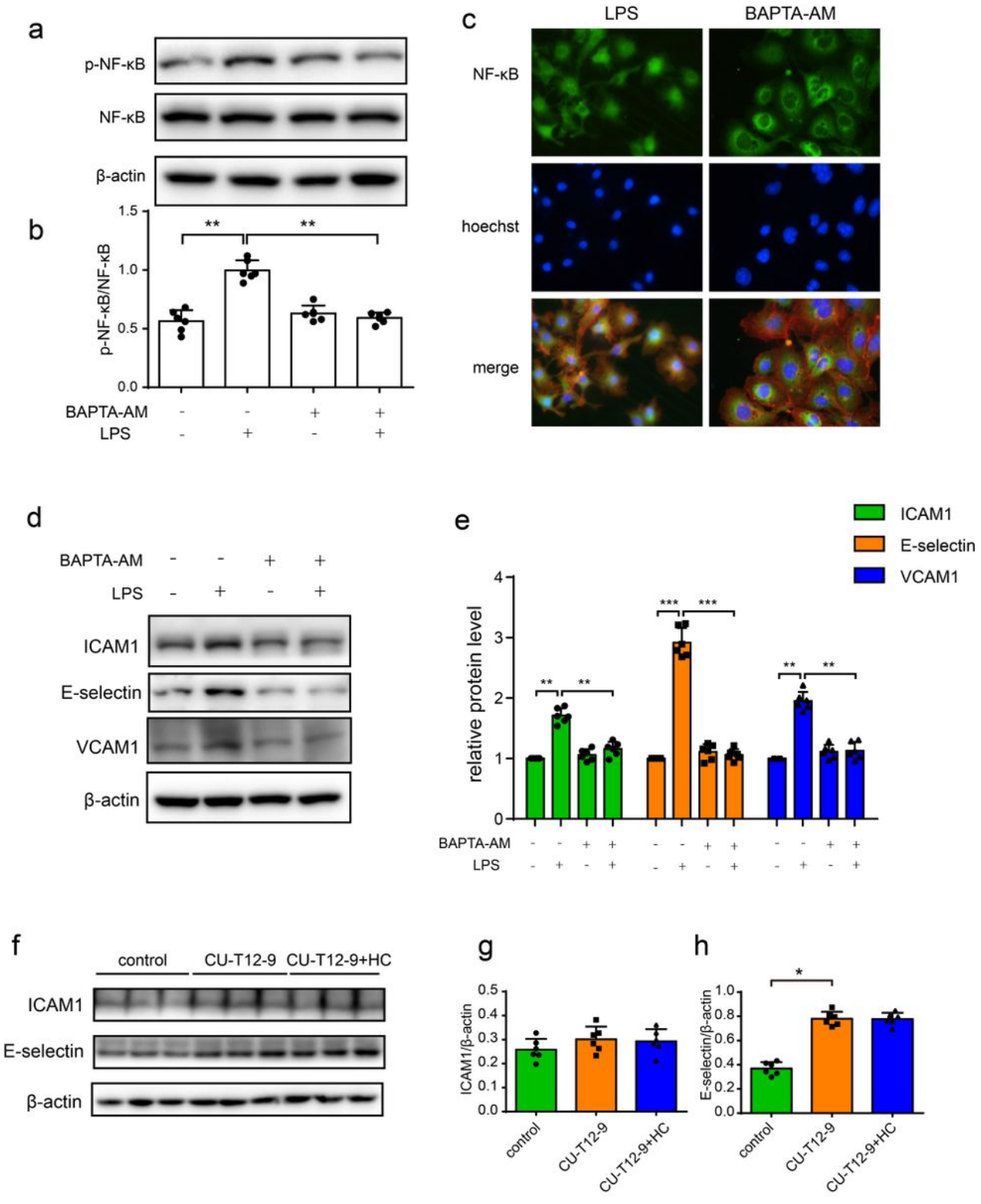

Figure 4

LPS signaling and NF-κB translocation are abrogated by clamping intracellular Ca2+. a, b. The protein level of p-NF-κB p65, NF-κB p65 was determined. Cells were treated as indicated. **P < 0.01, n = 6. c. Immunofluorescence staining of NF-κB was performed after treated with BPATA-AM. d, e The protein level

of VCAM1, ICAM1 and E-selectin was determined by western blot. Cells were loaded with BPATA-AM before stimulated by LPS (1μg/mL). **P < 0.01, n = 6. f-h. The protein level of ICAM1 and E-selectin was determined by western blot. Cells were treated with HC before stimulated by CU-T12-9(10μM). *P < 0.05, n = 6.

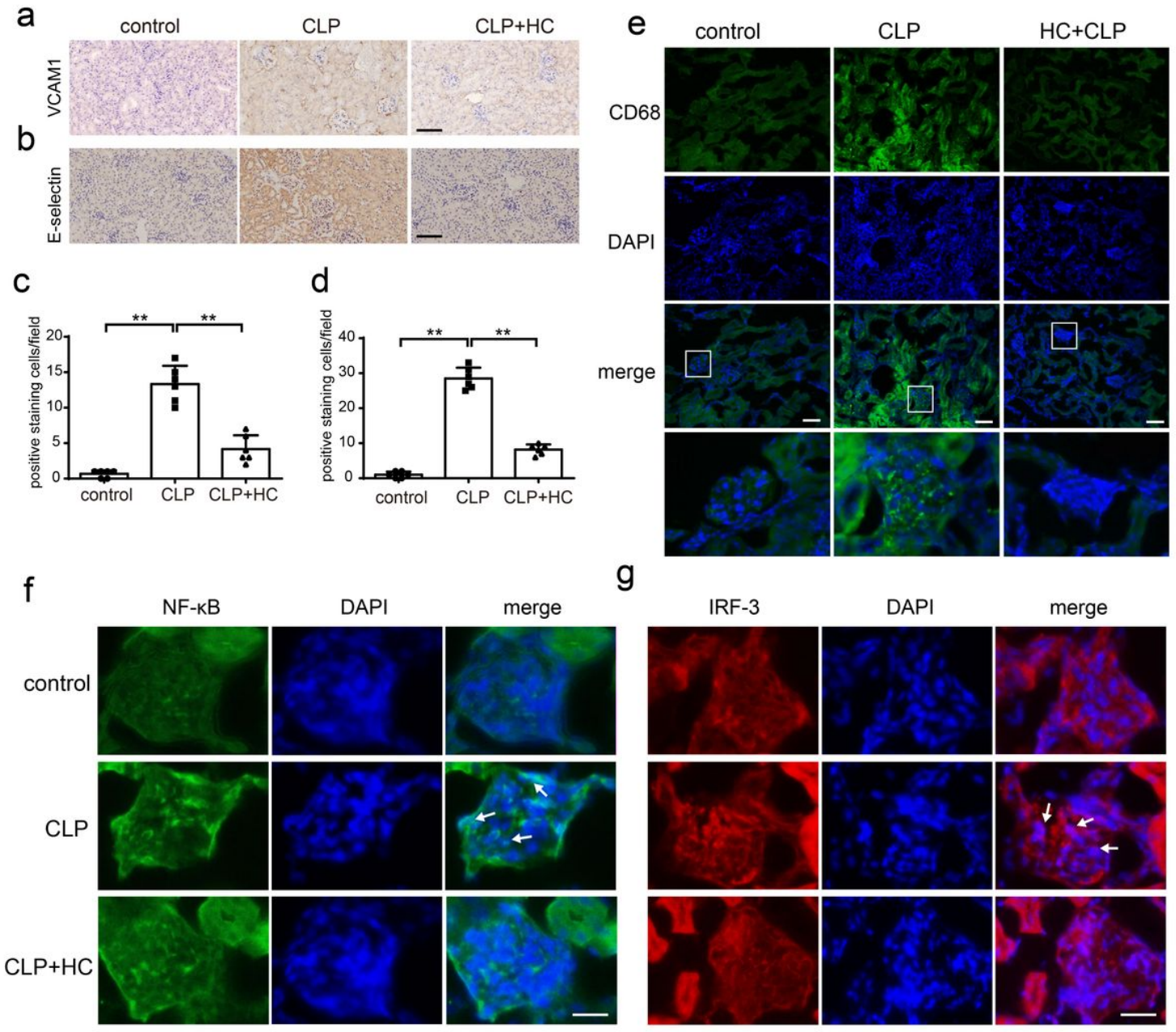

Figure 5

TRPV4 inhibition reduced glomerular endothelial inflammation and retained translocation of NF-κB and IRF-3 in vivo. a, b. The level of VCAM1and E-selectin was visualized using immunohistochemistry analysis in glomerulus after CLP. scale bar=100 μm. c, d Quantitative analysis of VCAM1and E-selectin positive cells in glomerulus. **P < 0.01, n = 6. e. Representative images showing the expression of CD68 in glomerulus. scale bar=100 μm. f, g. The expression of NF-κB and IRF-3 in glomerulus of mice. scale bar=50 μm.

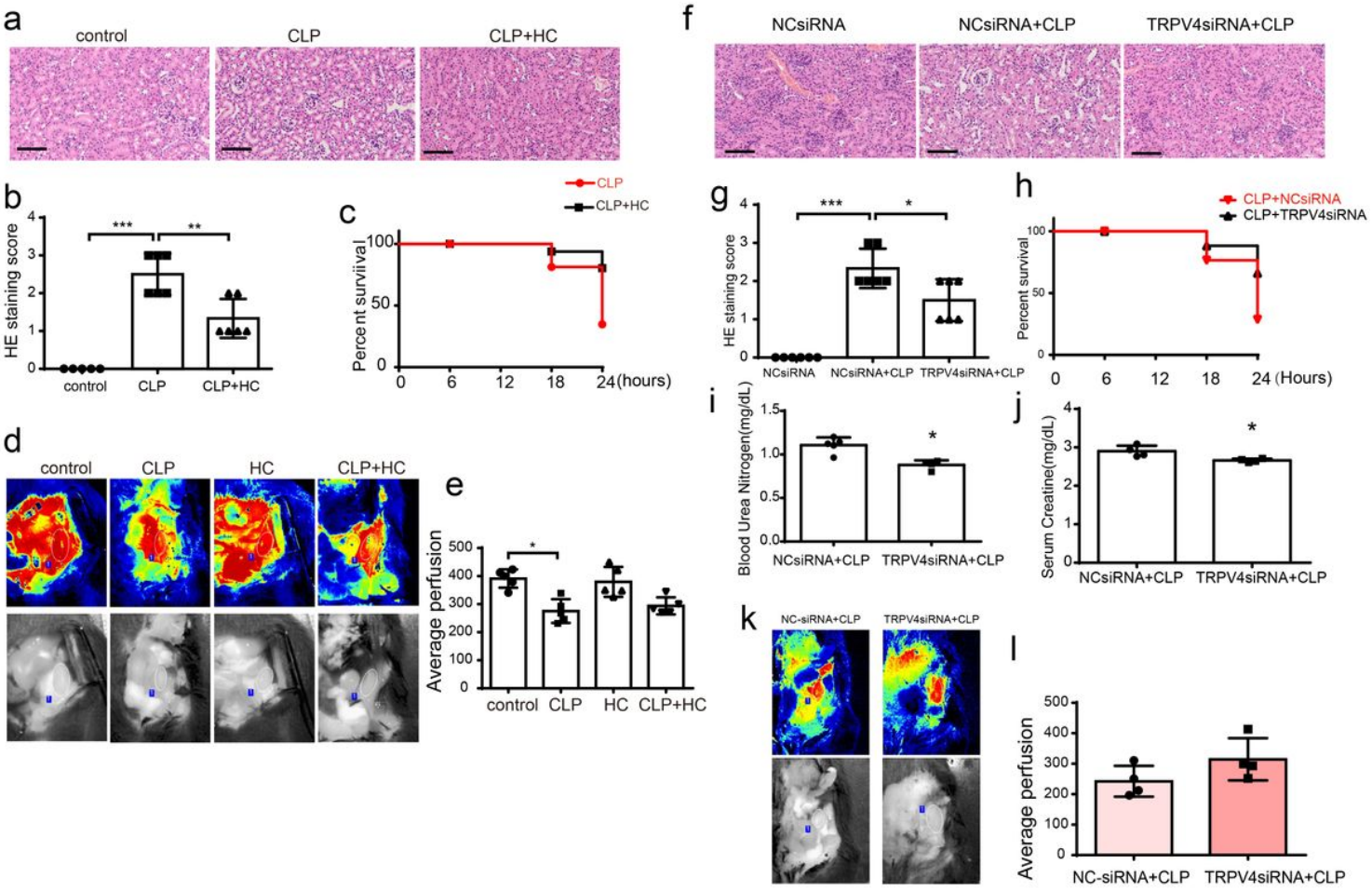

Figure 6

TRPV4 inhibition or knockdown of TRPV4 ameliorates CLP-induced kidney injury and renal vascular inflammation. HC (10mg/kg) was intraperitoneally injected 1 hour before CLP operation. a. Representative images of HE. Images were captured at magnification, ×200, scale bar=100 μm; b. Group data summarizes the results for HE staining scores. Histopathological grading of tissue injury was assessed using the 0- to 4-point scoring system. **P < 0.01, ***P < 0.001, n = 6. c. The survival rate of each group was recorded at 6, 12, 18 and 24 hours after CLP. d, e. 24 hours after CLP, renal blood flow was evaluated via laser doppler imaging and quantified as the average perfusion for each animal. *P < 0.05, n = 6. f. The NCsiRNA and TRPV4siRNA (5 mg/kg) were transfected in vivo via tail vein injection 3 days before CLP. Representative images of HE. Images were captured at magnification, ×200, scale bar=100 μm; g. Group data summarizes the results for HE staining scores. Histopathological grading of tissue injury was assessed using the 0- to 4-point scoring system. *P < 0.05, ***P < 0.001, n = 6. h. The survival rate of each group at 6, 12, 18 and 24 hours after CLP was recorded. i, j. Serum creatinine and urea nitrogen levels in mice of each group were measured 24 h after CLP. *P <0.05, n=6. k, l. renal blood flow was evaluated via laser doppler imaging and quantified as the average perfusion for each animal.

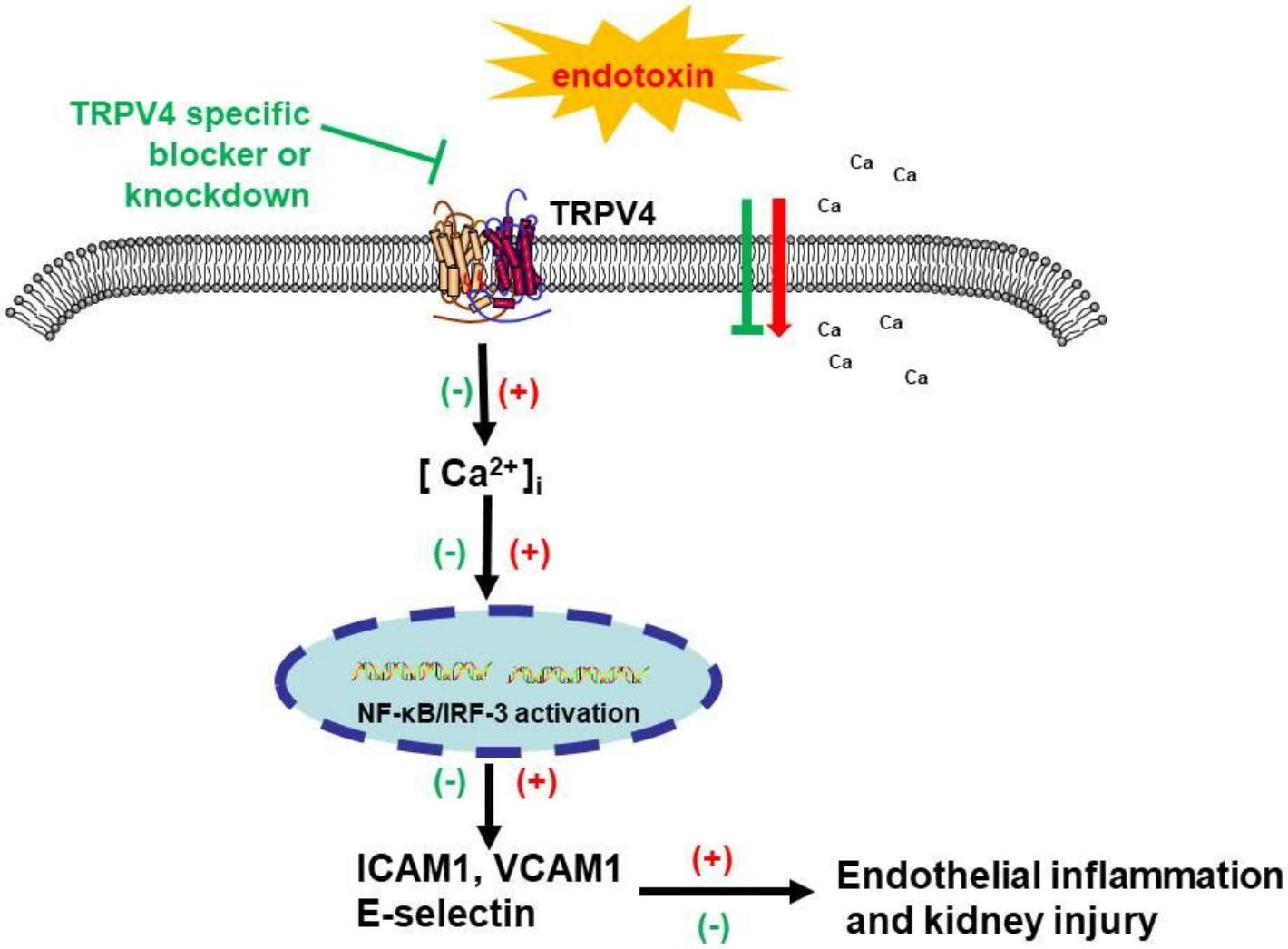

Figure 7

Schematic diagram of this study. Inhibition of TRPV4 ameliorates glomerular endothelial inflammation, kidney dysfunction, and increased mortality via mediating Ca2+ overload and NF-κB/IRF-3 activation.

Supplementary Files

This is a list of supplementary files associated with this preprint. Click to download.

- supplemental.pdf